Optimal Velocity and Power Split Control of Hybrid Electric Vehicles

***Abstract*—An assessment study of a novel approach is presented that combines discrete state-space Dynamic Programming and Pontryagin's Maximum Principle to gain optimal control of hybrid electric vehicles (HEV). In addition to the electric energy of the storage and the gear, the kinetic energy and the travel time are considered states in the problem. After presenting the corresponding model using a parallel HEV as an example, a benchmark method with Dynamic Programming is introduced which is used to show the solution quality of the novel approach. It is illustrated that the proposed method yields a close-to-optimal solution by solving the optimal control problem about one hundred thousand times faster than the benchmark method. This study paves the way for a development of a real-time application.**

I. Introduction

Hybrid Electric Vehicles (HEVs) are widely regarded as one of the most promising solutions to the mitigation of environmental issues caused by the ever-increasing usage of fossil fuels in transportation [17]. In addition to the internal combustion engine (ICE), HEV powertrains include one or more electric machines (EMs) and an electric storage, typically a battery. This provides an additional source of power for propulsion which can be exploited to decrease the fossil fuel consumption by 1) recuperating braking energy that can be stored in the battery for later use, 2) shutting down the ICE during idling and low power demands and 3) operating the ICE at more efficient load conditions by storing the excess energy in the battery [12].

The fuel consumption and energy efficiency of an HEV depend crucially on the energy management strategy (EMS). For a certain gas pedal position and energy state of the vehicle, the EMS determines the split of demanded power between the power sources (ICE and EMs). Additionally, it may choose the ICE on/off state as well as the gear selection for powertrains with an automated gearbox. HEVs equipped with a telemetry system may further improve the energy efficiency by planning the anticipated power split over a receding horizon in front of the vehicle.

Ample amount of scientific research has focused on the EMS that controls the three vehicle states, battery energy, gear and ICE on/off. Besides purely heuristic approaches, model-based control is the preferred scientific implementation since the EMS is coordinated by an optimal control algorithm. A comprehensive overview of different optimal, suboptimal and heuristic EMS for HEVs can be found in [18], [25].

Among the optimal control methods, Dynamic Programming (DP) is the one most commonly used ([23], [24], [29], [39], [40], [43], [47]) since DP can be easily applied to nonlinear, non-convex and mixed-integer control problems. However, a limitation of DP is the so-called *curse of dimensionality*, i.e. the computational effort increases exponentially with the number of state variables [1].

Thus, methods based on the Pontryagin's Maximum Principle (PMP) [34] have been proposed which adjoin the system dynamics to the objective. One of those well-known methods is the Equivalent Consumption Minimization Strategy (ECMS) [33] which simplifies the problem by neglecting the battery energy limits as well as by considering the gear and ICE on/off as control signals rather than state variables [6], [14], [22], [26], [30]. Other methods retain the battery energy constraints but require heuristics for the integer decisions. An example is the PMP method presented in [48] and the convex optimization methods proposed in [28], [36], [44].

To overcome the disadvantages of each single method, a combination of different optimization methods has also been suggested that typically separates the integer from the real-valued decisions. For instance, the approach in [31] combines DP and PMP by disregarding battery energy limits and regarding gear and ICE on/off as integer states. Similarly, [45] uses a combination of both methods to control the battery energy and the integer ICE on/off decision for a series hybrid bus and regards limits on the battery energy. Methods that combine convex optimization with either PMP or DP have been proposed in [8], [27], [32], [35]. There, battery energy limits are kept, and in case of a combination with DP, gear and ICE on/off can be considered integer states.

Besides the EMS, another factor that significantly affects the vehicle energy efficiency is the possibility to optimally control the kinetic and potential energy storage by varying the vehicle velocity in a hilly terrain while satisfying the travel time given. For instance, a more efficient driving can be achieved by decreasing velocity when climbing uphill and increasing velocity while rolling downhill instead of wasting energy at the braking pads.

In order to introduce methods for optimal control of the velocity, before coming to HEVs, publications which pay attention to conventional vehicles are presented. For instance, an early implementation for optimal velocity control of conventional passenger cars using DP for a real-time application was presented by Porsche, called ACC InnoDrive [37]. Other approaches using DP concentrate on controlling velocity on short-range trips, e.g. the distance between two traffic lights [7], [46]. Using DP for both velocity control and gear shifting of conventional trucks has been proposed in [15], [16]. Furthermore, DP is used for optimal velocity control of truck platoons [5]. But for the sake of computational efficiency, gear, ICE on/off and travel time are removed from the state vector, and the engine model is reduced to a simple constant efficiency.

Besides DP, other methods are examined for velocity control of conventional vehicles. For instance, convex quadratic programming has been proposed by [11]. A real-time capable, nonlinear predictive control approach for velocity control in urban areas is presented by [21]. Likewise, PMP can be used for velocity control. Early research calculating the optimal velocity of a conventional vehicle with PMP was done by [41].

In comparison to velocity control of conventional vehicles, the velocity control of HEVs is more challenging due to the higher number of states. This complex problem is still a current topic of research. A comprehensive overview of publications dealing with that topic can be found in [42].

Despite the high number of states, real-time control using DP is possible when, for instance, the prediction horizon is short [51]. Nonetheless, it is not the preferred approach due to the high computational load of having the two real-valued states (velocity and battery energy) and possibly the two integer states (gear and engine on/off). Bosch developed a system called Eco-ACC which uses DP for an offline calculation of deceleration trajectories when drawing near a slower vehicle in front [9]. The results of DP are used to obtain lookup tables for a control unit implementation.

Approaches for velocity control of HEV using methods other than DP is also possible such as the ACC system for HEV trucks, presented by [49] in which the author employs nonlinear optimization methods. In [50], a solution with PMP using a sum of piecewise affine continuous functions for HEV is presented. However, integer states are neglected and the model is restricted to strictly convex functions. Similarly, the procedure in [21] can be extended to control the power split in HEV as well. This method is used in [52] to optimize HEV trucks in a platoon.

Moreover, combinations of different methods are investigated. An approach, published recently, decouples the integer from the real-valued decisions, so that DP selects gear and powertrain mode while control of velocity and battery energy are chosen by convex optimization [19], [20]. However, model approximations may be required to derive a convex program [3].

In contrast, the paper at hand proposes a novel method for optimal control of velocity (kinetic energy), battery energy and gear of an HEV which does not require a convex model. Sampling is performed in the space coordinate along the traveled distance, which introduces the travel time as a fourth state in the problem and allows hilly terrain of any shape to be included directly in the problem. To overcome the high computational burden associated with the travel time as a state, the approach in the present paper combines DP and PMP. DP controls the vehicle's kinetic energy and gear, given the costates for battery energy and travel time; wherein the costates are obtained by applying the PMP. Similar to most ECMS approaches, the single shooting method is used to solve a two-point boundary value problem (BVP). This ensures that final constraints on the battery energy and the travel time are met.

As a result, the method introduced gives the same solution as a globally optimal DP when the battery is operated at nearly constant open circuit voltage and battery energy limits are not activated. However, for other operating conditions it has been observed that the proposed solution is nearly optimal, with about 0.59 ‰ higher fuel consumption than the benchmark solution for the sample horizon used.

This paper is organized as follows. The general optimal control problem is stated in Section II. Section III provides a benchmark solution obtained by solving a discrete state space DP. Section IV presents the proposed PMP-DP approach. Section V provides a case study in which the results of both the DP and the PMP-DP method are compared. Section VI comes to a conclusion and gives an outline of ongoing research in the field.

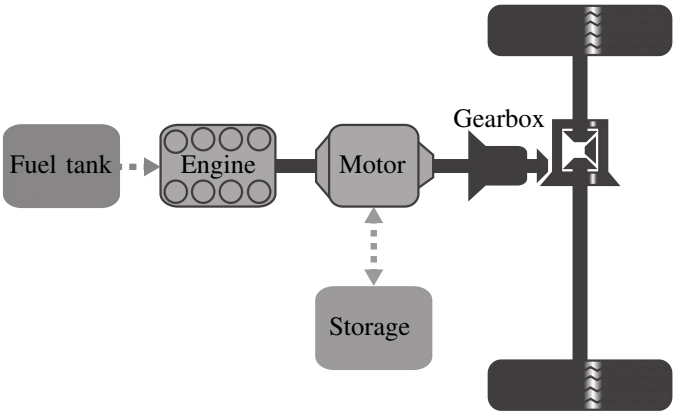

Fig. 1. Structure of a P2-HEV (according to [19]). It shows the energy flow from the fuel tank to the ICE which is connected with the EM. The storage delivers energy to the EM or receives energy from it. The torques of ICE and EM add up and are transmitted by the gearbox to the wheels.

II. Problem Description

In this section, the problem is formulated for optimal energy management of an HEV. The method proposed is presented for an HEV powertrain in a parallel configuration [12, p. 61]. However, it is straightforward to apply the method to other powertrain concepts.

A. Vehicle Model

The parallel HEV powertrain used in this study is illustrated in Fig. 1. The powertrain includes an ICE that converts chemical fuel energy to mechanical propulsion energy. The ICE is connected coaxially with an EM, which enables a hybrid mode of operation in which the ICE and the EM may split the necessary torque for propulsion. As energy storage an electric battery is used providing energy to the EM, when the EM is in motoring mode, and receiving energy when the EM is in generating mode. This enables recuperation of energy when the vehicle is braking (decreasing kinetic energy) or going downhill (decreasing potential energy), and storing of excess energy in the battery when the ICE is delivering more torque than needed. Conversely, the ICE can be supported by the EM using stored battery energy. Changing the ICE torque with the help of the EM may increase the ICE efficiency which is shown in Fig. 2.

Distributing the torque between ICE (T_E) and EM (T_M) is possible because they are connected directly, which also ensures an identical rotation speed

$$\omega(v, g) = \frac{v}{\mathrm{r}}\gamma(g) \tag{1}$$

which depends on the longitudinal vehicle velocity v, the dynamic rolling radius of the wheels r and the gear ratio $\gamma(g)$. The latter is determined by the gear g that is an integer system

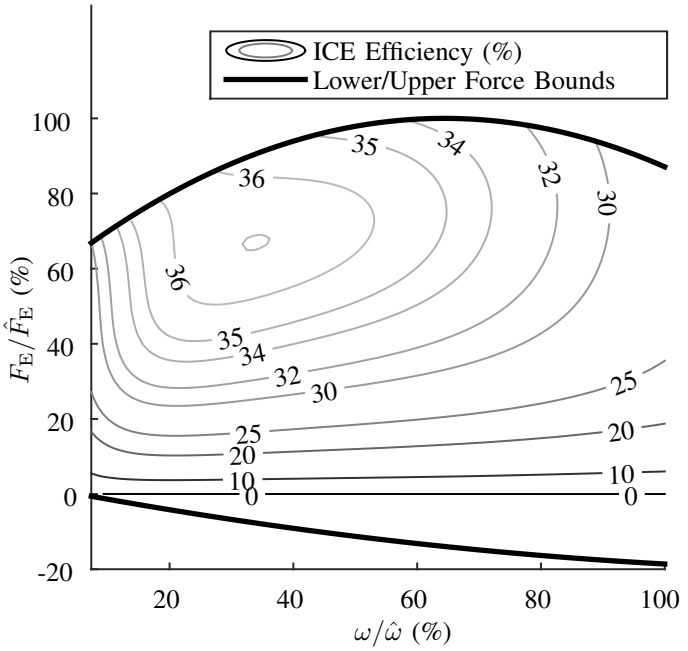

Fig. 2. Map of ICE efficiency and force bounds. Force and speed are given in terms of their maximum values $\hat{F}_E$ and $\hat{\omega}$.

state controlled by the signal u_g. The ICE force $F_E = T_E/r$, the EM force $F_M = T_M/r$ and the brake force F_B are control signals as well. They are gathered in the vector of continuous inputs

$$\mathbf{u}_c = (F_E, F_M, F_B), \tag{2}$$

which give the input vector

$$\mathbf{u} = (\mathbf{u}_c, u_g) \tag{3}$$

together with the integer signal u_g.

The forces F_E and F_M add up to a crankshaft force which the gearbox translates to a wheel force. The gearbox has an efficiency η_g that determines a dissipative force

$$F_{T,d}(\mathbf{u}) = \begin{cases} (F_M + F_E)(\eta_g - 1)/\eta_g, & \text{for } F_M + F_E \le 0 \\ (F_M + F_E)\eta_g, & \text{for } F_M + F_E > 0 \end{cases} \tag{4}$$

which counteracts the wheel force. The brake and the driving resistance due to inertia, air drag and road slope cause further retarding forces. Accordingly, the balance of forces at the wheel is

$$\mathrm{m}v\frac{dv}{ds} + \mathrm{c_a}v^2 + c_\alpha + F_B = (F_M + F_E - F_{T,d}(\mathbf{u}))\gamma(g) \quad \forall s \in [\mathrm{s_0}, \mathrm{s_f}], \tag{5}$$

where m is the vehicle mass, $\mathrm{c_a}$ is a constant for the air drag and c_α a slope-dependent factor. The balance is formulated in space coordinates s that reach from an initial position $\mathrm{s_0}$ to a final position $\mathrm{s_f}$. The term vdv/ds in (5) derives directly from the time to space transformation

$$\frac{dv}{dt} = v\frac{dv}{ds}. \tag{6}$$

Note that for brevity, the dependency of variables on s is not displayed anywhere and constants which do not depend on s are displayed in upright letters. For instance in (5) $\mathrm{c_a}$ does not depend on s while c_α does.

It can be noticed that the state dynamics in (5) are nonlinear. A straightforward way to remove nonlinearity, without introducing approximations, is to perform a variable change, where kinetic energy

$$E_V = \frac{1}{2}mv^2 \tag{7}$$

is used as system state instead of longitudinal velocity. In space domain, the derivative of vehicle energy transforms into

$$\frac{\partial E_V}{\partial s} = E_V' = \frac{1}{2}\mathrm{m}\frac{dv^2}{ds} = \mathrm{m}v\frac{dv}{ds} = \mathrm{m}vv'. \tag{8}$$

Consequently, (5) can be written as

$$E_V'(\mathbf{u}, E_V, g) = f_V(\mathbf{u}, E_V, g) = (F_M + F_E - F_{T,d}(\mathbf{u}))\gamma(g) - F_B - 2\mathrm{c_a}E_V/\mathrm{m} - c_\alpha \in \mathrm{m}[\mathrm{a_{min}}, \mathrm{a_{max}}], \tag{9}$$

which gives the state differential equation of the kinetic energy f_V that is limited by the minimal acceleration $\mathrm{a_{min}}$ and the maximal acceleration $\mathrm{a_{max}}$. The prime symbol ($'$) is used as a shorthand notation for the first derivative with respect to s.

Since the problem is formulated in space coordinates, the travel time t is introduced as a system state. Its state dynamics are expressed by the function

$$f_t(E_V) = t'(E_V) = 1/v = 1/\sqrt{2E_V/\mathrm{m}}. \tag{10}$$

The battery energy E_S is a fourth system state which is gathered with the other continuous states in the vector

$$\mathbf{x}_c = (E_S, E_V, t) \tag{11}$$

which is included in the state vector

$$\mathbf{x} = (\mathbf{x}_c, g) \tag{12}$$

together with the gear. This vector is used in the notation of the battery energy state dynamics

$$f_S(F_M, \mathbf{x}) = E_S'(F_M, \mathbf{x}) = -P_S(F_M, \mathbf{x})/\sqrt{2E_V/\mathrm{m}}, \tag{13}$$

where the chemical (i.e. internal) battery power P_S is considered to be negative when charging.

The battery is modeled as a series connection of an ideal voltage source and an ohmic resistance (cf. [12, p. 97]). Accordingly, the chemical power

$$P_S(F_M, \mathbf{x}) = P_{S,d}(F_M, \mathbf{x}) + P_{S,e}(F_M, \mathbf{x}) \in [\mathrm{P_{Smin}}, \mathrm{P_{Smax}}], \tag{14}$$

which is limited by the constant bounds $\mathrm{P_{Smin}}$ and $\mathrm{P_{Smax}}$, is the sum of the dissipative power $P_{S,d}$ and the battery terminal (electrical) power

$$P_{S,e}(F_M, \mathbf{x}) = P_M(F_M, \mathbf{x}) + P_{M,d}(F_M, \mathbf{x}) + P_A. \tag{15}$$

In (15), the sum of EM mechanical power is

$$P_M(F_M, \mathbf{x}) = T_M(F_M)\omega(\mathbf{x}) = F_M\sqrt{2E_V/\mathrm{m}}\gamma(g), \tag{16}$$

where P_A is the auxiliary power and $P_{M,d}(F_M, \mathbf{x})$ is the EM dissipative power which is given as a static lookup table.

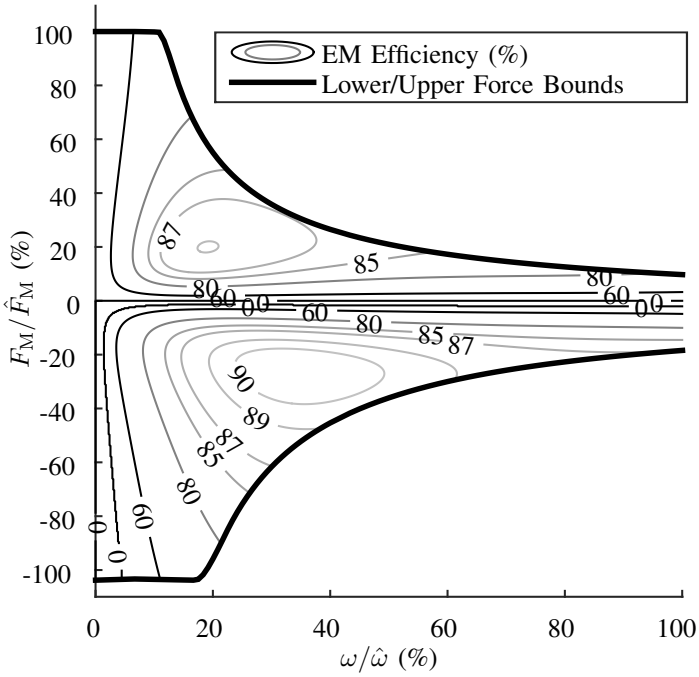

Fig. 3. Map of EM efficiency and force bounds. The force is given in terms of its maximum value $\hat{F}_M$.

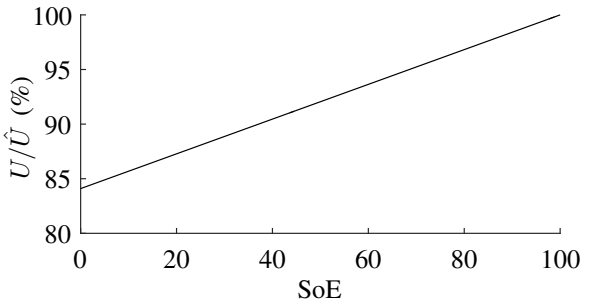

Fig. 4. Dependency of open-circuit voltage and the battery state of energy. The voltage is given in terms of its maximum value $\hat{U}$.

Providing a more informative depiction, the lookup table in Fig. 3 shows the EM efficiency.

The battery losses

$$P_{S,d}(F_M, \mathbf{x}) = \frac{\left(U(E_S) - \sqrt{U^2(E_S) - 4R(F_M, \mathbf{x})P_{S,e}(F_M, \mathbf{x})}\right)^2}{4R(F_M, \mathbf{x})} \quad (17)$$

depend on the terminal power, the battery resistance $R(F_M, \mathbf{x})$ and the open-circuit voltage $U(E_S)$ which is illustrated in Fig. 4. The abscissa shows the battery's state of energy (SoE), i.e. the battery energy normalized with respect to its maximum value. The resistance

$$R(F_M, \mathbf{x}) = \begin{cases} R_+, & \text{for } P_S(F_M, \mathbf{x}) \leq 0 \\ R_-, & \text{for } P_S(F_M, \mathbf{x}) > 0 \end{cases} \quad (18)$$

may change value, depending on whether the battery is being charged or discharged.

B. Problem Formulation

This section formulates the optimal control problem using the previously introduced model.

Observing constraints, the objective is to minimize the fuel consumption for a given slope profile. The amount of fuel expressed as consumed fuel energy is the integrated sum of F_E and the dissipative ICE force $F_{E,d}(F_E, \mathbf{x})$ over s. Similarly to F_M, a lookup table provides $F_{E,d}(F_E, \mathbf{x})$ which is connected to the ICE efficiency shown in Fig. 2. Besides the fuel energy, the objective function includes a term that penalizes gear changes. Hence, the optimal control problem is

$$\text{minimize} \int_{s_0}^{s_f} ((F_E + F_{E,d}(F_E, \mathbf{x}))\gamma(g) + |u_g|\beta)\, ds \quad (19a)$$

$$= \int_{s_0}^{s_f} \mathcal{L}(\mathbf{u}, \mathbf{x}) ds \quad (19b)$$

s.t.

$$\mathbf{x}_c' = \mathbf{f}_c(\mathbf{u}, \mathbf{x}) \quad (19c)$$

$$g^+ = g + u_g \quad (19d)$$

$$\mathbf{x}(s_0) = \mathbf{x}_0, \quad \mathbf{x}(s_f) = \mathbf{x}_f \quad (19e)$$

$$\mathbf{x} \in [\mathbf{x}_{min}, \mathbf{x}_{max}] \quad (19f)$$

$$\mathbf{u}_c \in [\mathbf{u}_{c,min}(\mathbf{x}), \mathbf{u}_{c,max}(\mathbf{x})] \quad (19g)$$

$$u_g \in \{-1, 0, 1\}, \quad (19h)$$

where β represents a value for the loss in energy and comfort when shifting gear ($u_g \neq 0$).

In problem (19), the function

$$\mathbf{f}_c(\mathbf{u}, \mathbf{x}) = (f_S, f_V, f_t) \quad (20)$$

combines the state dynamics of the continuous states. Furthermore, the gear at the next instance is g^+. The initial and final state conditions are given by the vectors $\mathbf{x}_0$ and $\mathbf{x}_f$, respectively. Due to technological reasons, the state space is bounded by lower ($\mathbf{x}_{min}$) and upper ($\mathbf{x}_{max}$) limits. While the limits of E_S and g are constant, the bounds of E_V and t depend on s. Note that the limits of travel time and the bounds on kinetic energy depend on each other. For instance, the upper limit of t can be derived from the lowest possible velocity, i.e. the lower bound on E_V and vice versa.

Similar to the states, the continuous inputs have lower and upper bounds expressed by $\mathbf{u}_{c,min}(\mathbf{x})$ and $\mathbf{u}_{c,max}(\mathbf{x})$, respectively. The bounds on the ICE force and the EM force shown in Fig. 2 and Fig. 3, respectively, depend on $\omega(v, g)$, and consequently, on the states E_V and g. In contrast, the third continuous input $F_B \in [0, \text{inf}]$ has constant limits.

III. Discrete State Space DP

This section presents a benchmark solution of problem (19), calculated by implementing a discrete state space DP, which guarantees a globally optimal solution.

A. Discrete Problem Formulation

The hybrid (mixed-integer) control problem (19) is here transformed to a purely integer problem by discretization of the travel distance and quantization of the values of the

continuous states $\mathbf{x}_\mathrm{c}$. For brevity, symbols used for continuous signals in (19) represent discrete signals hereafter.

Thus, the discrete problem formulation is

$$\text{minimize} \sum_{k=1}^{N_\mathrm{k}} (\mathcal{L}(\mathbf{x},\mathbf{u})\Delta s \tag{21a}$$

s.t.

$$\mathbf{x}_\mathrm{c}(k+1) = \mathbf{x}_\mathrm{c}(k) + \mathbf{f}_\mathrm{c}(\mathbf{u},\mathbf{x})\Delta s \tag{21b}$$
$$g(k+1) = g(k) + u_\mathrm{g} \tag{21c}$$
$$\mathbf{x}(0) = \mathbf{x}_0, \quad \mathbf{x}(N_\mathrm{k}) = \mathbf{x}_\mathrm{f} \tag{21d}$$
$$\mathbf{x} \in \{\mathbf{x}_\mathrm{min}, \mathbf{x}_\mathrm{min} + \Delta\mathbf{x}, ..., \mathbf{x}_\mathrm{max}\} \tag{21e}$$
$$\mathbf{u}_\mathrm{c} \in [\mathbf{u}_\mathrm{c,min}(\mathbf{x}), \mathbf{u}_\mathrm{c,max}(\mathbf{x})] \tag{21f}$$
$$u_\mathrm{g} \in \{-1, 0, 1\}, \tag{21g}$$

in which k denotes a discrete point of s with the constant step size Δs between two points and the final point N_k. The feasible sets of the states are quantized to get uniform grids. The quality of the solution depends on the state quantization $\Delta\mathbf{x}$. A finer quantizing of the state space leads to a solution closer to the continuous optimum but exponentially increases the computational effort of the DP implementation.

B. Implementation

DP uses Bellman's Principle of Optimality [1], i.e. it computes the optimal solution by splitting the problem into subproblems. The principle states that when a trajectory Π from an initial state to a final state is optimal, a trajectory from any intermediate state on Π to the final state is also optimal as well as a trajectory from the initial state to any intermediate state on Π. This means that DP can be computed forward or backward in time (or more precisely in space, for problem formulation (19)). For basic information on DP, please see [2].

In this paper, the DP algorithm is implemented in forward direction utilizing MATLAB[1], i.e. the algorithm starts with $k = 1$ going forward searching the optimal predecessor state k for every state at $k+1$ yielding the optimal state transition. By inverting the state dynamics, the control signals are obtained. This is realized using nested loops which iterate all feasible state values $\mathbf{x}(k+1)$ and calculate the transition from all feasible $\mathbf{x}(k)$ by iterating $E_\mathrm{V}(k)$, $E_\mathrm{S}(k)$ and $g(k)$. In contrast, the travel time

$$t(k) = t(k+1) - \Delta s / \sqrt{2E_\mathrm{V}(k)/m} \tag{22}$$

is computed directly. However, if $t(k)$ does not match with a discrete point in the time-state grid it is rounded to the nearest higher value, which will lead to a discretization error. Thus, a small quantization step size of the travel time is selected allowing the results to be used as a benchmark for the novel approach which is introduced hereafter.

IV. PMP-DP Approach

In this section problem (19) is formulated using PMP. Subsequently, an approach is proposed that combines PMP and DP.

[1]MATLAB is a registered trademark of The MathWorks, Inc.

A. PMP formulation of the problem

Following Pontryagin's maximum principle, problem (19) can be solved by formulating the Hamiltonian

$$\mathcal{H}(\mathbf{x},\boldsymbol{\psi},\mathbf{u}) = \mathcal{L}(\mathbf{x},\mathbf{u}) + \boldsymbol{\psi}^\mathrm{T}(s)\,\mathbf{x}_\mathrm{c}'(s), \tag{23}$$

where, the vector of Lagrange multipliers

$$\boldsymbol{\psi} = (\psi_\mathrm{S}, \psi_\mathrm{V}, \psi_\mathrm{t}) \tag{24}$$

includes the costates ψ_S, ψ_V and ψ_t which relate to the continuous states E_S, E_V and t in (21), respectively. Hence, the problem is reformulated to

$$\text{minimize} \quad \mathcal{H}(\mathbf{x},\boldsymbol{\psi},\mathbf{u}) \tag{25a}$$

s.t.

$$\psi' = -\frac{\partial\mathcal{H}(\mathbf{x},\boldsymbol{\psi},\mathbf{u})}{\partial\mathbf{x}_\mathrm{c}} \tag{25b}$$
$$g(k+1) = g(k) + u_\mathrm{g} \tag{25c}$$
$$\mathbf{x}(0) = \mathbf{x}_0, \quad \mathbf{x}(N_\mathrm{k}) = \mathbf{x}_\mathrm{f} \tag{25d}$$
$$\mathbf{x} \in \{\mathbf{x}_\mathrm{min}, \mathbf{x}_\mathrm{min} + \Delta\mathbf{x}, ..., \mathbf{x}_\mathrm{max}\} \tag{25e}$$
$$\mathbf{u}_\mathrm{c} \in [\mathbf{u}_\mathrm{c,min}(\mathbf{x}), \mathbf{u}_\mathrm{c,max}(\mathbf{x})] \tag{25f}$$
$$u_\mathrm{g} \in \{-1, 0, 1\}. \tag{25g}$$

where (25b) is a necessary condition that has to be fulfilled at the optimum in the case where state constraints (25e) are not activated [10], [13]. The objective function changes from the Lagrange resolvent (19a) to a local minimization of the Hamiltonian (25a). Additionally, the state dynamics (21b) are replaced by the adjoint differential equation (25b) which has to be solved to determine the costate dynamics.

The necessary condition (25e) can be used to derive some important properties of the costate dynamics. Under the assumption that the battery voltage variation (see Fig. 4) can be neglected [12, p. 214] and state constraints do not get activated, the battery costate would satisfy

$$\psi_\mathrm{S}' = -\frac{\partial\mathcal{H}(\mathbf{x},\boldsymbol{\psi},\mathbf{u})}{\partial E_\mathrm{S}} \approx 0. \tag{26}$$

Thus, ψ_S can be seen as constant, i.e. one scalar value for the costate can be found to obtain a suboptimal control trajectory that satisfies the final constraint on the battery energy. However, with a constant ψ_S it cannot be assured that the boundary constraints on the battery energy are fulfilled. This problem is approached by some authors by means of an iterative search method that splits the horizon into segments with a constant value for the costate as soon as the state boundary is reached. The resulting solution is a piecewise constant battery costate, which has been proven in [48] to be the optimal solution for certain types of convex energy management problems. For generally non-convex problems, as problem (21), it has been observed that the piecewise constant solution is close to the optimum [22].

Similarly to ψ_S, the costate for the travel time is constant because its differential equation

$$\psi_\mathrm{t}' = -\frac{\partial\mathcal{H}(\mathbf{x},\boldsymbol{\psi},\mathbf{u})}{\partial t} = 0 \tag{27}$$

is not dependent on the travel time. Moreover, following (10), the travel time is monotonically increasing and its state bounds are activated only at the beginning and the end of the horizon, so a horizon split is not necessary.

In contrast to ψ_t, the costate for the kinetic energy ψ_V is not constant and there are no known approximations that can be used to obtain a close-to-optimal costate trajectory. The dynamic equation

$$\begin{aligned}\psi_\mathrm{V}'(\mathbf{x},\boldsymbol{\psi},\mathbf{u}) &= -\frac{\partial \mathcal{H}}{\partial E_\mathrm{V}} \\ &= \frac{\partial}{\partial E_\mathrm{V}} F_\mathrm{E,d}\gamma(g) \\ &- \psi_\mathrm{S}\,\frac{\partial P_\mathrm{S,e}}{\partial E_\mathrm{V}}\,\frac{U}{\sqrt{2E_\mathrm{V}/m}\sqrt{U^2-4RP_\mathrm{S,e}}} \\ &- \psi_\mathrm{S}\,\frac{1}{4R}U\sqrt{U^2-4RP_\mathrm{S,e}-U} \\ &- \psi_\mathrm{V}\,2\mathrm{c_a}/m \\ &- \psi_\mathrm{t}\,\frac{1}{2}(2E_\mathrm{V}/m)^{-\frac{3}{2}}\end{aligned} \tag{28}$$

depends on all states but the travel time. For reasons of readability, the dependencies are omitted in (28).

As a consequence to (28), it is not easy to determine the costates for problem (25) with a single shooting method which is a common approach for similar problems (e.g. ECMS). Therefore, the following subsection introduces an approach to overcome this obstacle.

B. Algorihm of PMP-DP Approach

The idea behind the novel approach is to use a Hamiltonian as objective function for a discrete state space DP, where the states for battery energy and for travel time are replaced by costates (ψ_S and ψ_t). Since the costates are (piecewise) constant, the values that will solve the BVP can be found by a shooting method. The corresponding approach is shown in Fig. 5, where first the problem

$$\text{minimize} \sum_{k=1}^{N_\mathrm{k}} \mathcal{H}(\mathbf{x},\boldsymbol{\psi},\mathbf{u}) \tag{29a}$$

$$= \sum_{k=1}^{N_\mathrm{k}} \mathcal{L}(\mathbf{x},\mathbf{u}) + \psi_\mathrm{S}\,E_\mathrm{S}' + \psi_\mathrm{t}\,t' \tag{29b}$$

s.t.

$$E_\mathrm{V}(k+1) = E_\mathrm{V}(k) + f_\mathrm{V}\Delta s \tag{29c}$$

$$g(k+1) = g(k) + u_\mathrm{g} \tag{29d}$$

$$\mathbf{x}(0) = \mathbf{x}_0, \quad \mathbf{x}(N_\mathrm{k}) = \mathbf{x}_\mathrm{f} \tag{29e}$$

$$\mathbf{x} \in \{\mathbf{x}_\mathrm{min}, \mathbf{x}_\mathrm{min} + \Delta\mathbf{x}, ..., \mathbf{x}_\mathrm{max}\} \tag{29f}$$

$$\mathbf{u}_\mathrm{c} \in [\mathbf{u}_\mathrm{c,min}(\mathbf{x}), \mathbf{u}_\mathrm{c,max}(\mathbf{x})] \tag{29g}$$

$$u_\mathrm{g} \in \{-1, 0, 1\} \tag{29h}$$

is solved for initially guessed values for ψ_t and ψ_S.

Afterwards, a subprogram solves the BVP for the whole horizon without constraints on E_S. Therefor, ψ_t is iterated using the bisection method until $t(N_\mathrm{k}) \approx t_\mathrm{f}$, where t_f is the final constraint on the travel time. Subsequently, ψ_S is found

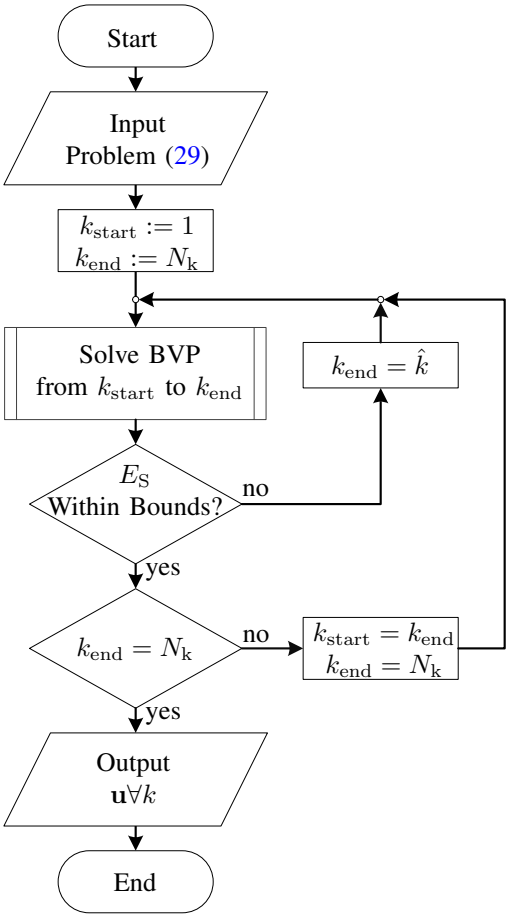

Fig. 5. Algorithm of PMP-DP approach.

in the same way. It is not always possible to exactly meet the final constraints because of non-linearities in the model, which is, for instance, discussed in [31]. Hence, the subprogram exits after a finite number of iterations and selects the solution closest to the final constraints.

If E_S computed by the subprogram is not within the state limits for all k, the segments final point k_end is set to $\hat{k}$ which is the point at which the limits are exceeded the most. At $\hat{k}$, the final state condition is set to the respective limit. If E_S of the shorter segment violates the state bounds again, the segment is split again in two parts and the procedure repeats. Otherwise, the next decision block checks whether the current segment is the last. If this is not the case, the segment from the actual k_end to the final point of the horizon will be computed and if necessary split again. The process is continued until the control trajectory for the whole horizon is calculated.

The DP used to solve problem (29) is implemented in MATLAB, similarly to the benchmark solution described in Secion III-B. The difference is that the DP in this case has only two states, E_V and g. This decreases the computational effort of the DP significantly, which is pointed out in the following Section V.

V. Results

This section presents a comparison of the benchmark solutions gained from DP (Section III) and the PMP-DP approach

TABLE I
STATE QUANTIZATION FOR SIMULATION.

State	Step Size	Grid Points	
t	0.01 s	4949	(only DP)
E_S	5 kJ	271	(only DP)
E_V	5 kJ	25	
g	1	6	

(Section IV). The results show that the PMP-DP method obtains a solution that is close to the global optimum obtained by DP but with a significantly lower computational effort.

The sample data used for the comparison was recorded during a test drive with a passenger car on a randomly selected interurban route in Germany. The car's navigation system provides prediction data specified by the Advanced Driver Assistance Systems Interface Specifications (ADASIS) protocol [4], [38] to the vehicle bus. ADASIS includes information about velocity restrictions, curvature and slope for an upcoming horizon of 8.2 km at maximum.

The restrictions on velocity and the maximal apex speed are used to compute an upper kinetic energy state bound. To obtain the lower bound, 120 kJ are subtracted which corresponds to a deviation of about 9 km/h when the upper velocity limit is 100 km/h.

For the simulation, the horizon is discretized with a step size of 10 m and the states are quantized with the values shown in Table I. Note that the travel time state with its large number of grid points has the biggest impact on the computational time of the DP. Fine quantization is selected to keep the discretization error of t small.

The error done by using the approximation (26) is small for a narrow operating range of the battery which is typically the case for short horizons. Due to this, at first both methods are compared for a distance of 1000 m. The respective simulation results are shown in Fig. 6. Here, the upper three plots illustrate the behavior of the system states. The kinetic energy state is represented by the velocity shown in the top plot together with state bounds and the road altitude. The second plot from the top shows that battery energy limits are not activated and the voltage (SoE) is nearly constant. Hence, the simulation of both methods yield the same results.

That the results match can be reasserted by comparing the costates of both solutions. Deriving exact costate values for the benchmark solution is not possible, due to the error caused by discretization. Instead, uncertainty regions are obtained, where the uncertainty bounds for the costates can be derived for the globally optimal solution [18, p. 88]. For instance, the boundaries of the battery energy costate can be computed using

$$\frac{\mathbf{K}_{\mathrm{E}_\mathrm{S}^*,\mathrm{k}} - \mathbf{K}_{\mathrm{E}_\mathrm{S}^*+\Delta\mathrm{E}_\mathrm{S},\mathrm{k}}}{\Delta E_\mathrm{S}} \leq \psi_\mathrm{S}(k) \leq \frac{\mathbf{K}_{\mathrm{E}_\mathrm{S}^*,\mathrm{k}} - \mathbf{K}_{\mathrm{E}_\mathrm{S}^*-\Delta\mathrm{E}_\mathrm{S},\mathrm{k}}}{-\Delta E_\mathrm{S}}. \tag{30}$$

Here, $\mathbf{K}$ is the cost matrix of the DP, the index E_S^* denotes the optimal battery energy, and ΔE_S is the sample step size of the battery energy. It is shown in the bottom two plots of Fig. 6 that the costates used for the PMP-DP approach lie in between the uncertainty region. Because of the sparsely populated cost matrix at the simulation start, the error of the bounds is large but gets smaller when preceding in space.

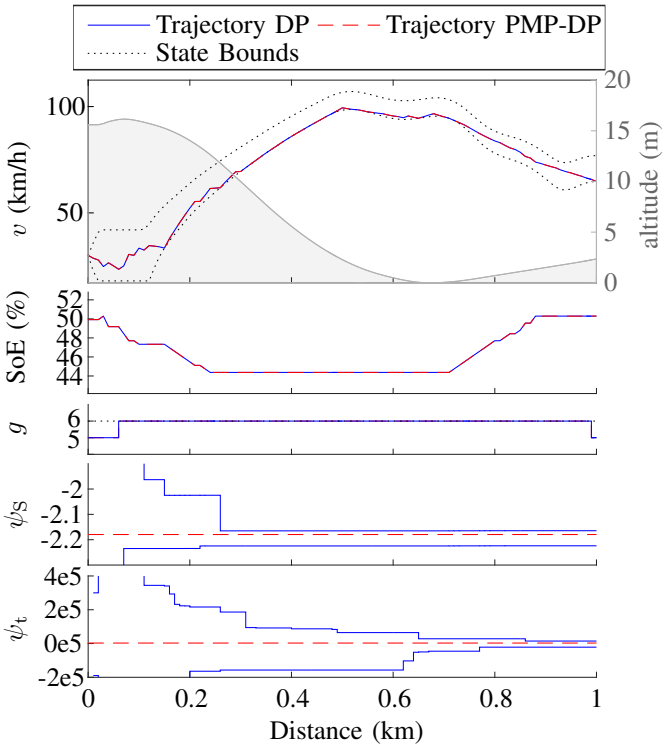

Fig. 6. Comparison of both methods for 1000 m. The system states, shown in the upper three plots, are equal because only a small window of the battery energy is used, i.e. the voltage is nearly constant what is assumed for the PMP-DP approach and the battery energy is far from the limits which are 0 % and 100 %. The lower two plots confirm this by showing the costates used for PMP-DP (dashed line) and the uncertainty bounds calculated with DP (solid line). When preceding in space, the boundaries enclose the constant costates which shows that the assumption (26) in this case does not lead into error.

When calculating longer horizons, the activation of the battery energy limits and the non-constant battery voltage introduce discrepancies between the proposed and the benchmark solution. Nevertheless, the results computed by the two approaches for the full horizon are similar. This is shown in Fig. 7, where it can be observed that the error caused by neglecting the dependency between the battery voltage and SoE (using a piecewise constant value for ψ_S) is relatively small. Additionally, it can be seen that the segmentation explained in Section IV-B leads to a behavior of ψ_S which can be comprehended when observing the uncertainty bounds. Note that the constant value for ψ_t is still in between the uncertainty bounds.

Accordingly, the close-to-optimal solution of the PMP-DP increases fuel consumption by 0.59 ‰. The differences of the velocity and battery energy trajectories are 1.23 % and 2.76 % NRMSD which is the root-mean-square deviation normalized to the respective difference between the maximum and minimum value.

However, much higher difference can be observed between the computation times. While the full horizon of the globally

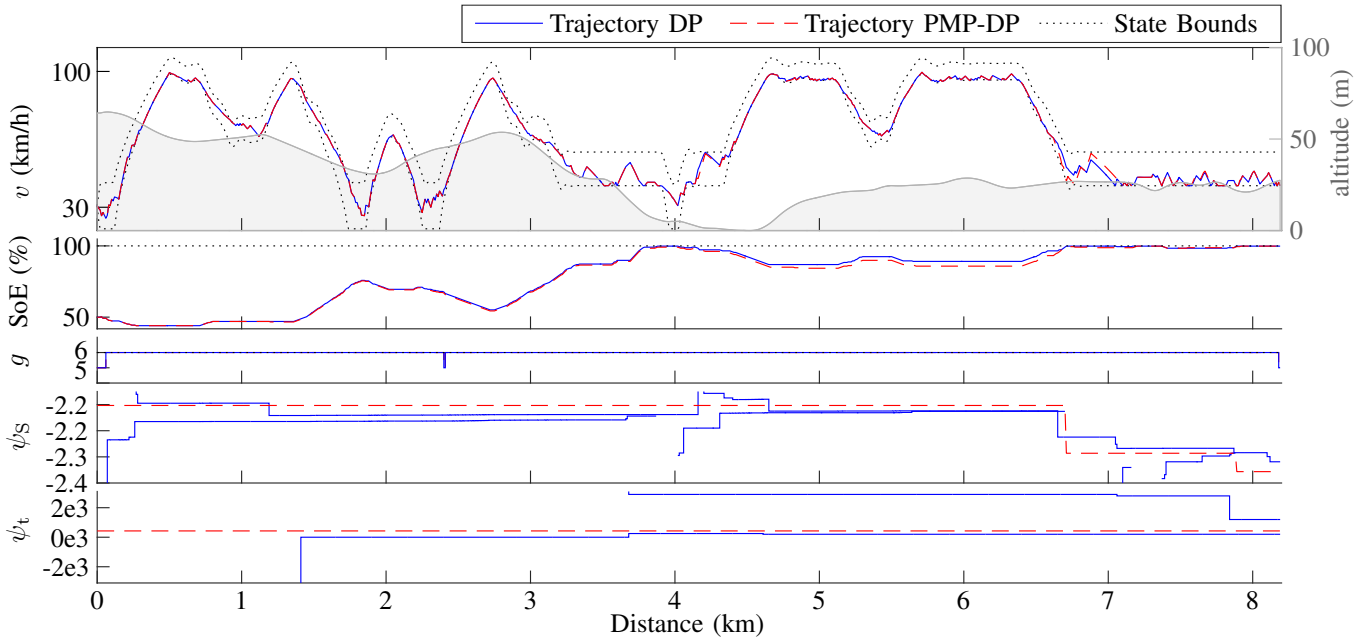

Fig. 7. Comparison of both approaches for the full horizon. Despite the same final state conditions, there are slight differences between both results. This is due to the assumption of a piecewise constant costate for the battery energy. It can be seen that ψ_S is frequently out of the calculated uncertainty area. However, the costate shows a similar behavior. For instance, at about 6.7 km the state boundaries are hit, and ψ_S jumps down as well as the upper uncertainty bound. The induced error causes the fuel consumption of the PMP-DP to increase by 0.59 ‰ as well as a NRMSD of 1.23 % and 2.76 % for the velocity and the SoE, respectively.

optimal DP was calculated on a high performance computer[2] in about 56 days, the PMP-DP only takes about 60 s on a personal computer[3]. The PMP-DP needs 9 iterations for solving the unconstrained full horizon BVP and then divides the horizon into 3 segments from which each one needs 4 iterations to be solved. Additionally, to assess the computational effort in a real-time environment, the method is implemented in a rapid prototyping control unit[4] which does not support multicore computation. As a result, the computation time is 40 seconds for only one iteration of the BVP solver for the full horizon.

As a consequence of the computational effort, a real-time use of PMP-DP in its present form is not possible. Since lowering the effort by increasing the step size of E_V (cf. Table I) is not a good option because the discretization error will enlarge and the solution will move away from the continuous globally optimal one, other possibilities are mentioned in the following final chapter.

VI. Conclusion and Future Research

This paper presents an approach that combines DP and PMP in a new way. It solves the four state mixed-integer problem about one hundred thousand times faster than a pure DP implementation which was used as a benchmark but has nearly the same solution quality. However, a real-time implementation is not possible at the moment.

Due to this, future research will focus on decreasing the computational effort by approximating the derivation of the kinetic energy costate. Additionally, the effect will be studied of including the integer decisions as control signals, rather than states.

[2]One node with 24 cores (Intel E5-2690) and 5 GB RAM per Core were used on the Bull HPC-Cluster (Taurus) at The Center for Information Services and High Performance Computing (ZIH) at Technische Universität Dresden

[3]A Lenovo Thinkpad T430s with an Intel Core i5-3320M and 16 GB RAM is used.

[4]DSpace MicroAutoboxII

References

[1] R. Bellman, "The theory of dynamic programming," *Bull. Amer. Math. Soc.*, pp. 503–515, 1954, 6, ISSN: 0002-9904.

[2] D. P. Bertsekas, *Dynamic programming and optimal control*, 3rd ed, ser. Athena Scientific optimization and computation series. Belmont, Mass.: Athena Scientific, 2005-2007, 47 pp., ISBN: 1-886529-26-4.

[3] S. Boyd and L. Vandenberghe, *Convex Optimization*. Cambridge University Press, 2004, ISBN: 0521833787.

[4] A. Bracht, *ADASIS v2 Protocol, Version 2.03.0*, 2013.

[5] L. Bühler, "Fuel-Efficient Platooning of Heavy Duty Vehicles through Road Topography Preview Information," KTH, Stockholm, Sweden, 2013.

[6] S. Delprat, J. Lauber, T. M. Guerra, and J. Rimaux, "Control of a parallel hybrid powertrain: optimal control," *IEEE Transactions on Vehicular Technology*, vol. 53, pp. 872–881, 3 2004.

[7] W. Dib, L. Serrao, and A. Sciarretta, Eds., *Optimal control to minimize trip time and energy consumption in electric vehicles*, Vehicle Power and Propulsion Conference (VPPC), 2011 IEEE, presented at the Vehicle Power and Propulsion Conference (VPPC), 2011 IEEE, 2011, 1-8.

[8] P. Elbert, T. Nüesch, A. Ritter, N. Murgovski, and L. Guzzella, "Engine On/Off Control for the Energy Management of a Serial Hybrid Electric Bus via Convex Optimization," *IEEE Transactions on Vehicular Technology*, vol. 63, pp. 3549–3559, 8 2014.

[9] F. Flehmig, F. Kästner, K. Knödler, and M. Knoop, "Eco-ACC für Elektro- und Hybridfahrzeuge," *ATZ - Automobiltechnische Zeitschrift*, vol. 116, pp. 22–27, 4 2014, ISSN: 0001-2785.

[10] O. Föllinger, *Optimale Regelung und Steuerung*. München Wien: R. Oldenbourg Verlag, 1994, 197 pp.

[11] S. Gonsrang, "Optimization-based Energy Management System for Pure Electric Vehicles," in *Energy Efficient Vehicles 2015*, vol. 5, pp. 100–110.

[12] L. Guzzella and A. Sciarretta, *Vehicle propulsion systems, Introduction to modeling and optimization*, 2nd ed. Berlin and London: Springer, 2007, 345 pp., ISBN: 978-3-540-74691-1.

[13] Hans Peter Geering, *Optimal Control with Engineering Applications*. Berlin Heidelberg: Springer-Verlag, 2007.

[14] M. Helbing, "Energiemanagement für eine parallele Hybridarchitektur," diploma thesis, Technische Universität Dresden, Dresden, 2014, 128 pp.

[15] E. Hellström, J. Aslund, and L. Nielsen, "Design of an efficient algorithm for fuel-optimal look-ahead control," *Control Engineering Practice*, vol. 18, pp. 1318–1327, 11 2010, ISSN: 0967-0661.

[16] E. Hellström, M. Ivarsson, J. Aslund, and L. Nielsen, "Look-ahead control for heavy trucks to minimize trip time and fuel consumption," *Control Engineering Practice*, vol. 17, pp. 245–254, 2 2009, ISSN: 0967-0661.

[17] P. Hofmann, *Hybridfahrzeuge, Ein alternatives antriebssystem für die zukunft*, 2. Auflage. 2014, 560 pp., ISBN: 978-3-7091-1779-8.

[18] B. d. Jager, T. van Keulen, and J. Kessels, *Optimal control of hybrid vehicles*, ser. Advances in industrial control. London and New York: Springer, 2013, 158 pp., ISBN: 978-1-4471-5075-6.

[19] L. Johannesson, N. Murgovski, E. Jonasson, J. Hellgren, and B. Egardt, "Predictive energy management of hybrid long-haul trucks," *Control Engineering Practice*, vol. 41, pp. 83–97, 2015, ISSN: 0967-0661.

[20] L. Johannesson, M. Nilsson, and N. Murgovski, Eds., *Look-ahead vehicle energy management with traffic predictions*, vol. 48, Columbus, Ohio, USA, 2015, 244-251.

[21] Kamal, M. A. S., M. Mukai, J. Murata, and T. Kawabe, "Model Predictive Control of Vehicles on Urban Roads for Improved Fuel Economy," *Control Systems Technology, IEEE Transactions on*, vol. 21, pp. 831–841, 3 2013, ISSN: 1063-6536.

[22] S. Kutter and B. Bäker, Eds., *An iterative algorithm for the global optimal predictive control of hybrid electric vehicles*, Vehicle Power and Propulsion Conference (VPPC), 2011 IEEE, presented at the Vehicle Power and Propulsion Conference (VPPC), 2011 IEEE, 2011, 1-6.

[23] S. Kutter, "Eine prädiktive und optimierungsbasierte Betriebsstrategie für autarke und extern nachladbare Hybridfahrzeuge," Dissertation, Technische Universität Dresden, Dresden, 2013.

[24] K.-Y. Liang, J. Mårtensson, and K. H. Johansson, "Power Management Strategy for a Parallel Hybrid Electric Truck," *IEEE Transactions on Intelligent Transportation Systems*, 2003, ISSN: 1524-9050.

[25] A. A. Malikopoulos, "Supervisory Power Management Control Algorithms for Hybrid Electric Vehicles: A Survey," *IEEE Transactions on Intelligent Transportation Systems*, vol. 15, pp. 1869–1885, 5 2014, ISSN: 1524-9050.

[26] S. Mulder, "Energy Management Strategy for a Hybrid Container Crane," Master Thesis, Delft University of Technology, Delft, 2009, 77 pp.

[27] N. Murgovski, L. M. Johannesson, and J. Sjoberg, "Engine On/Off Control for Dimensioning Hybrid Electric Powertrains via Convex Optimization," *Vehicular Technology, IEEE Transactions on*, vol. 62, pp. 2949–2962, 7 2013, ISSN: 0018-9545.

[28] N. Murgovski, L. Johannesson, J. Sjöberg, and B. Egardt, "Component sizing of a plug-in hybrid electric powertrain via convex optimization," *Mechatronics*, vol. 22, pp. 106–120, 1 2012.

[29] N. Murgovski, J. Sjöberg, and J. Fredriksson, "A methodology and a tool for evaluating hybrid electric powertrain configurations," *Int. J. Electric and Hybrid Vehicles*, vol. 3, pp. 219–245, 3 2011.

[30] C. Musardo, G. Rizzoni, Y. Guezennec, and B. Staccia, "A-ECMS: An Adaptive Algorithm for Hybrid Electric Vehicle Energy Management," *European Journal of Control*, vol. 11, pp. 509–524, 4–5 2005, ISSN: 0947-3580.

[31] Ngo Dac Viet, "Gear Shift Strategies for Automotive Transmissions," PhD thesis, Eindhoven University of Technology, Eindhoven, 2012, 202 pp.

[32] T. Nüesch, P. Elbert, M. Flankl, C. Onder, and L. Guzzella, "Convex Optimization for the Energy Management of Hybrid Electric Vehicles Considering Engine Start and Gearshift Costs," *Energies*, vol. 7, p. 834, 2 2014, ISSN: 1996-1073.

[33] G. Paganelli, T. M. Guerra, S. Delprat, J.-J. Santin, M. Delhom, and E. Combes, "Simulation and assessment of power control strategies for a parallel hybrid car," *Proceedings of the Institution of Mechanical Engineers, Part D: Journal of Automobile Engineering*, vol. 214, pp. 705–717, 7 2000, ISSN: 0954-4070.

[34] L. S. Pontryagin, V. G. Boltyanskii, R. V. Gamkrelidze, and E. F. Mishchenko, *The Mathematical Theory of Optimal Processes*. New York - London - Sydney: Interscience Publishers, 1962.

[35] M. Pourabdollah, N. Murgovski, B. S. Egardt, and A. Grauers, "An Iterative Dynamic Programming/convex Optimization Procedure for Optimal Sizing and Energy Management of PHEVs," in *The 19th World Congress of the International Federation of Automatic Control*, pp. 6606–6611.

[36] M. Pourabdollah, N. Murgovski, A. Grauers, and B. Egardt, "Optimal sizing of a parallel PHEV powertrain," *IEEE Transactions on Vehicular Technology*, vol. 62, pp. 2469–2480, 6 2013.

[37] T. Radke, *Energieoptimale Längsführung von Kraftfahrzeugen durch Einsatz vorausschauender Fahrstrategien*, Dissertation. Karlsruhe: KIT Scientific Publishing, 2013, 220 pp., ISBN: 978-3-7315-0069-8.

[38] C. Ress, D. Balzer, A. Bracht, S. Durekovic, and J. Löwenau, *ADASIS PROTOCOL FOR ADVANCED IN-VEHICLE APPLICATIONS*, 2008.

[39] A. A. Robichek, E. J. Elton, and M. J. Gruber, "DYNAMIC PROGRAMMING APPLICATIONS IN FINANCE," *The Journal of Finance*, vol. 26, pp. 473–506, 2 1971, ISSN: 1540-6261.

[40] Rui Wang and S. M. Lukic, Eds., *Dynamic programming technique in hybrid electric vehicle optimization*, Electric Vehicle Conference (IEVC), 2012 IEEE International, presented at the Electric Vehicle Conference (IEVC), 2012 IEEE International, 2012, 1-8.

[41] A. B. Schwarzkopf and R. B. Leipnik, "Control of highway vehicles for minimum fuel consumption over varying terrain," *Transportation Research*, vol. 11, pp. 279–286, 4 1977.

[42] A. Sciarretta, G. D. Nunzio, and L. L. Ojeda, "Optimal Ecodriving Control: Energy-Efficient Driving of Road Vehicles as an Optimal Control Problem," *IEEE Control Systems Magazine*, vol. 35, pp. 71–90, 5 2015.

[43] O. Sundstrom and L. Guzzella, Eds., *A generic dynamic programming Matlab function*, Control Applications, (CCA) & Intelligent Control, (ISIC), 2009 IEEE, presented at the Control Applications, (CCA) & Intelligent Control, (ISIC), 2009 IEEE, 2009, 1625-1630.

[44] E. D. Tate and S. P. Boyd, Eds., *Finding Ultimate Limits of Performance for Hybrid Electric Vehicles*, 2000.

[45] C. Tempelhahn, S. Uebel, and B. Bäker, "State of the art in optimal control of series hybrid electric vehicles taking account of driveability," in *Proceedings EEHE Wiesloch 2016*.

[46] P. Themann, A. Zlocki, and L. Eckstein, "Energieeffiziente Fahrzeuglängsführung durch V2X-Kommunikation," *ATZ - Automobiltechnische Zeitschrift*, vol. 116, pp. 62–67, 7-8 2014, ISSN: 0001-2785.

[47] S. Uebel, C. Tempelhahn, M. Liebers, S. Kutter, and B. Bäker, "Anwendung der Variationsrechnung für Steuerungsaufgaben im Kraftfahrzeug," vol. 62, 2014, 4.

[48] T. van Keulen, J. Gillot, B. d. Jager, and M. Steinbuch, "Solution for state constrained optimal control problems applied to power split control for hybrid vehicles," *Automatica*, vol. 50, pp. 187–192, 1 2014, ISSN: 0005-1098.

[49] T. van Keulen, B. d. Jager, D. Foster, and M. Steinbuch, Eds., *Velocity trajectory optimization in hybrid electric trucks*, Marriott Waterfront, Baltimore, MD, USA, 2010, 5074-5079.

[50] T. van Keulen, B. d. Jager, and M. Steinbuch, Eds., *Optimal Trajectories for Vehicles with Energy Recovery Options*, Milan, Italy, 2011, 3831-3836.

[51] H.-G. Wahl, K.-L. Bauer, F. Gauterin, and M. Holzapfel, Eds., *A real-time capable enhanced dynamic programming approach for predictive optimal cruise control in hybrid electric vehicles*, Intelligent Transportation Systems - (ITSC), 2013 16th International IEEE Conference on, presented at the Intelligent Transportation Systems - (ITSC), 2013 16th International IEEE Conference on, 2013, 1662-1667.

[52] K. Yu, Q. Liang, J. Yang, and Y. Guo, "Model predictive control for hybrid electric vehicle platooning using route information," *Proceedings of the Institution of Mechanical Engineers, Part D: Journal of Automobile Engineering*, pp. 1–13, 2015, ISSN: 0954-4070.